

PENETRATIVE CONVECTION DUE TO INTERNAL HEATING IN A ROTATING MAGNETIC NANOFUID LAYER WITH VARIABLE GRAVITY EFFECT

M. Arora and M.K. Sharma

MSC 2010 Classifications: 76W05, 76U05, 76R10.

Keywords: Magnetic nanofluids, Variable gravity, Rotation, Penetrative convection.

Abstract The present numerical work explores the influence of rotation on penetrative thermal convection at the onset in magnetic nanofluid (\mathcal{MG}_{fluid}), purely driven by internal heating, under the action of variable gravity conditions. The analysis is restricted to a thin layer of *water based magnetic nanofluid* ($\mathcal{W}\text{-}\mathcal{MG}_{fluid}$) and *ester based magnetic nanofluid* ($\mathcal{E}\text{-}\mathcal{MG}_{fluid}$), in which three modes—Brownian diffusion, thermophoresis, and magnetophoresis—are identified as critical components of the convective process. The Chebyshev pseudospectral method has been utilized as a computational technique to precisely assess stability criteria and pinpoint the critical conditions marking the onset of convection. This approach enables an exact analysis of the eigenvalue problem, central in the framework of the theory of linear stability. By means of this approach, critical conditions for the onset of convection may be determined within the study, and how these conditions vary with different varied physical parameters may be ascertained. The discussion focuses on rotational speed, the intensity of internal heating, and the variable gravitational field acting on these physical parameters, which may influence the onset of convection via neutral stability curves ($\mathcal{N}_s\text{Curves}$) and critical stability curves ($\mathcal{C}_s\text{Curves}$). To this aim, relevant parameters such as Taylor number, Rayleigh number, Langevin parameter, modified diffusivity ratios, Lewis number, and concentration Rayleigh number are investigated to understand their contribution to the \mathcal{MG}_{fluid} . These results give detailed information about the coupled interaction of these parameters and enhance predictive capabilities regarding the convection behavior of the \mathcal{MG}_{fluid} in applications.

1 Introduction

\mathcal{MG}_{fluid} , colloidal suspensions comprising magnetic nanoparticles dispersed in a carrier liquid, have garnered considerable attention for their exceptional thermal conductivity and sensitivity to magnetic fields. Their ability to modulate heat transfer and fluid flow under magnetic influence has led to widespread applications across various fields, including cooling systems, biomedical technology, and energy devices [1]. When exposed to complex environments, such as a rotating medium with variable gravity and internal heat sources, the convective behavior of these nanofluids becomes highly intricate. Investigating the onset of convection in such conditions is crucial for advancing theoretical knowledge and practical applications relevant to geophysical, astrophysical, and industrial settings.

Research on thermal instability in ferromagnetic fluids was pioneered by Sekar and Vaidyanathan [2]. They explored how ferromagnetic fluids behave under rotation about a vertical axis in the presence of a vertical magnetic field. Using the Brinkman model with free-free boundary conditions, they discovered that the stability of the system is enhanced in scenarios with low permeability and high rotational speeds. This study laid the groundwork for further exploration into how factors such as medium permeability and rotation affect the stability of ferromagnetic fluids in porous environments. Building upon these findings, Sunil and Mahajan [3] extended the analysis by examining nonlinear stability in magnetized ferrofluids heated from below in a rotating porous medium. Their study, which used stress-free boundary conditions, revealed the presence of subcritical instabilities, underscoring the complex interaction between magnetic and buoyancy forces. The results showed that rotation has significant effects on both linear and nonlinear stability, offering deeper insight into the dynamics of ferrofluids in rotating systems.

Buongiorno's foundational work on convective transport in nanofluids identified critical slip mechanisms, including Brownian motion and thermophoresis, as drivers of nanoparticle movement [4]. Following this, Nield and Kuznetsov [5] investigated instability onset in nanofluid-saturated porous media, considering both non-oscillatory and oscillatory convection patterns. Their theoretical framework provided a new perspective on nanofluid behavior in porous systems. Later, refining the model with more realistic boundary conditions, they found that oscillatory convection is unlikely under these constraints [6]. This advancement contributed significantly to the understanding of nanofluids in porous environments. Further expanding on nanofluid instability, Bhadauria and Agarwal [7] analyzed thermal instability in a rotating porous medium saturated with nanofluid, with particular focus on nanoparticle distribution. Their research, grounded in both linear and nonlinear stability theories, demonstrated that rotational effects, quantified by the Taylor number, play a stabilizing role, especially in scenarios with high rotation. This study highlighted the necessity of considering both nanoparticle distribution and rotational forces when assessing nanofluid stability in porous media. For additional insights, see [8, 9, 10].

The influence of internal and external heating on convection in porous media has been a longstanding area of research. Early studies by Gasser and Kazimi [11] using linear stability theory revealed that convection could be driven by either internal heating or heating from below. Ames and Cobb [12] expanded this area by examining penetrative convection induced by internal heating alone in porous media. Utilizing linear and nonlinear approaches, they elucidated the conditions that lead to convective initiation, providing foundational insights into convection driven by internal heat sources. Related research can be found in [13, 14, 15, 16, 17]. In more recent work, Yadav et al. [18] investigated convection driven by internal heating in a rotating, nanofluid-saturated porous medium using the Brinkman model. Their study demonstrated how internal heating and rotational effects interplay to drive convective processes in complex systems. Similarly, Nanjundappa et al. [19] studied penetrative ferroconvection in a porous layer under a uniform vertical magnetic field. Employing the Brinkman-extended Darcy model, they analyzed how magnetic forces and internal heating influence the convection patterns in such systems,

enriching our understanding of ferrofluid behavior in magnetized and rotating porous media.

Gravity variations with height is a significant factor in large-scale natural convection processes such as oceanic and atmospheric convection affect the dynamics of convection in ways often neglected in laboratory conditions, where gravity is assumed constant. Rionero and Straughan [14] explored the role of variable gravity in natural convection within porous media, discovering that gravity variations could instigate convection when coupled with an internal heat source, thereby opening new avenues for understanding convection in porous environments. Subsequent research by Alex and Patil [21] examined double-diffusive convection within isotropic porous layers, focusing on gravity's influence. Their findings contributed to understanding the role of gravity variations in complex systems. Kaloni and Qiao [22] further advanced this research using energy methods to analyze the nonlinear stability of convection under variable gravity, incorporating an inclined temperature gradient to illustrate how varying gravitational conditions affect convection patterns. More recent studies, such as those by Chand et al. [23, 24], examined variable gravity's effects on convection in nanofluid-saturated porous layers, integrating particle dynamics like Brownian motion and thermophoresis into the analysis. Their work provided a comprehensive view of how gravity variations and nanoparticle interactions influence convection, especially under rotational forces in nanofluid systems.

This study aims to explore the onset of penetrative convection driven by internal heating in a rotating, magnetic-fluid-saturated medium, with a particular focus on variable gravity effects. The investigation centers on a thin horizontal layer exposed to both internal heat sources and external magnetic fields, analyzing the impact of parameters such as the Taylor number, Rayleigh number, Langevin parameter, modified diffusivity ratios, Lewis number, and concentration Rayleigh number on the initiation and behavior of penetrative convection. By examining these factors in detail, this study seeks to deepen our understanding of how internal heating and magnetic influences interact to shape convection in magnetized fluid systems.

2 Geometrical Configuration

An infinite horizontal layer of incompressible magneto-gravitational fluid permeates a medium uniformly throughout the domain $z \in [0, d]$. The fluid is assumed to be incompressible, simplifying the governing equations by eliminating density variations. This configuration facilitates the study of flow dynamics and stability under the combined effects of magnetic fields and gravitational forces, providing resistance and influencing permeability and convection. Here, the gravity g acting downward, the magnetic field, $\mathbf{H} = H_0^{ext} \mathbf{k}$, is applied vertically, and the system rotates around the z -axis with angular velocity $\Omega = (0, 0, \Omega)$. Convection is driven by an internal heat source of strength Q (see Figure 1).

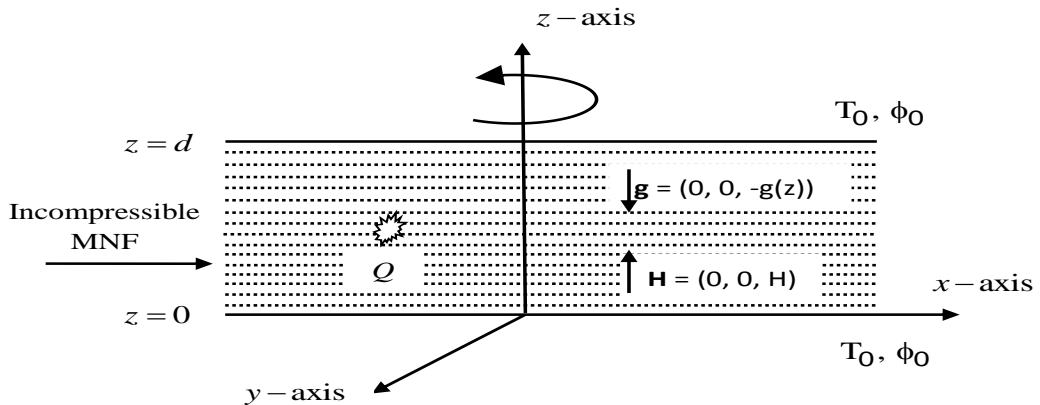


Figure 1. Geometric configuration of the problem

3 Formulation

Building upon the formulations provided in [4], [25], [26] and [27], we derive the governing equations for the system using the Boussinesq approximation. This approximation allows for the simplification of the momentum, continuity, and energy equations by assuming that density variations are only significant in the buoyancy term. These equations incorporate the combined influences of thermal, buoyancy, and magnetic effects, which are essential for examining the convective stability of the fluid.

$$\nabla \cdot \mathbf{u} = 0. \quad (3.1)$$

$$\rho_f \left(\frac{\partial \mathbf{u}}{\partial t} + \mathbf{u} \cdot \nabla \mathbf{u} \right) = -\nabla p + \mu \nabla^2 \mathbf{u} + \mu_0 (M \cdot \nabla) \mathbf{H} - \rho g (1 + \epsilon h(z)) \mathbf{k} + 2\rho_f (\mathbf{u} \times \Omega), \quad (3.2)$$

$$\frac{\partial \phi}{\partial t} + \mathbf{u} \cdot \nabla \phi = \nabla \cdot \left(D_B \nabla \phi + D_T \frac{\nabla T}{T_0} - D_H \nabla H \right). \quad (3.3)$$

$$(\rho c)_f \left(\frac{\partial T}{\partial t} + \mathbf{u} \cdot \nabla T \right) = \nabla \cdot (k_1 \nabla T) + \rho_p c_p (D_B \nabla T \cdot \nabla \phi + D_T \frac{\nabla T \cdot \nabla T}{T_0} - D_H \nabla T \cdot \nabla H) + Q, \quad (3.4)$$

$$\nabla \cdot \mathbf{B} = 0, \quad \nabla \times \mathbf{H} = 0, \quad \mathbf{B} = \mu_0(\mathbf{M} + \mathbf{H}). \quad (3.5)$$

$$\mathbf{M}_{eq} = \frac{\mathbf{H}}{H} [M_0 + \chi(H - H_0) - K_m(T - T_0) + K_p(\phi - \phi_0)]. \quad (3.6)$$

The boundary conditions (bc_s) can be expressed as

$$w = 0, \quad T = T_0, \quad \phi = \phi_0 \quad \text{at } z = 0 \quad \text{and} \quad \text{at } z = d, \quad (3.7)$$

Applying a dimensionless transformation to equations (3.1)–(3.6) yields the following system of equations.

$$\nabla \cdot \mathbf{u} = 0, \quad (3.8)$$

$$\frac{1}{Pr} \left(\frac{\partial \mathbf{u}}{\partial t} + \mathbf{u} \cdot \nabla \mathbf{u} \right) = -\nabla p + \nabla^2 \mathbf{u} + \lambda_1 (\mathbf{M} \cdot \nabla) \mathbf{H} - (Rn\phi - T + Ra_N N_\phi T \phi - \rho_1 \phi + \rho_2) s(z) \mathbf{k} + Ta^{1/2} (\mathbf{u} \times \mathbf{k}), \quad (3.9)$$

$$\frac{\partial \phi}{\partial t} + \mathbf{u} \cdot \nabla \phi = \frac{1}{Le} \nabla^2 \phi + \frac{Na}{Le} \nabla^2 T - \frac{Na'}{Le} \nabla^2 H, \quad (3.10)$$

$$\frac{\partial T}{\partial t} + \mathbf{u} \cdot \nabla T = \nabla^2 T + \frac{Nb}{Le} (\nabla T \cdot \nabla \phi) + \frac{NaNb}{Le} (\nabla T \cdot \nabla T) - \frac{Na'Nb}{Le} (\nabla T \cdot \nabla H) + 2Ra, \quad (3.11)$$

$$\chi_2 \nabla \cdot \mathbf{M} + \nabla \cdot \mathbf{H} = 0, \quad (3.12)$$

$$\mathbf{M} = \frac{\mathbf{H}}{H} (1 + \chi) \left\{ \frac{\chi}{1 + \chi} H - \frac{M_1}{M_3} T + \frac{M'_1}{M'_3} \phi + \frac{\chi_2 - \chi}{1 + \chi} \right\}, \quad (3.13)$$

$$\text{where } \lambda_1 = \frac{\mu_0 M_0 H_0 K}{\kappa \mu}, \quad \rho_1 = \frac{g \alpha \rho_f d^3 \phi_0 T_0}{\kappa \mu}, \quad \rho_2 = \frac{g \rho_f d^3 (1 + \alpha T_0)}{\kappa \mu},$$

$$Ra_N = 1 - \phi_0, \quad N_\phi = \frac{\phi_0}{1 - \phi_0}, \quad s(z) = 1 + \epsilon h(z).$$

The dimensionless parameters introduced are as follows:

$$Pr = \frac{\mu}{\rho_f \kappa}, \quad Rn = \frac{(\rho_p - \rho_f) \phi_0 g d^3}{\mu \kappa}, \quad Le = \frac{\kappa}{D_B}, \quad Ra = \frac{\rho_f g \alpha Q d^5}{2 \mu \kappa k_1}, \quad Ta = \frac{4 \Omega^2 d^4}{\nu^2}$$

$$M_1 = \frac{\mu_0 \mu \kappa \chi^2 H_0^2}{(\rho_f g \alpha T_0)^2 d^4 (1 + \chi)}, \quad M'_1 = \frac{\mu_0 \chi^2 H_0^2}{\rho_f g \alpha d (1 + \chi) \phi_0}, \quad M_3 = \frac{\mu_0 \chi H_0^2}{\rho_f g \alpha d T_0},$$

$$M'_3 = \frac{\mu_0 \chi H_0^2}{\rho_f g \alpha d \phi_0}, \quad Nb = \frac{(\rho c)_p}{(\rho c)_f} \phi_0, \quad Na = \frac{\mu \kappa D_T}{\rho_f g \alpha \phi_0 d^3 D_B T_0}, \quad Na' = \frac{D_H H_0}{D_B \phi_0}.$$

Here Pr : Prandtl number, Rn : concentration Rayleigh number, Le : Lewis number, Ra : Rayleigh number, Ta : Taylor number, M_1, M'_1, M_3, M'_3 are the magnetic parameters, Nb is the modified particle-density increment and Na, Na' are the modified diffusivity ratios. The bc_s (3.7) in non-dimensional form become

$$w = 0, \quad T = \frac{\rho_f g \alpha d^3 T_0}{\mu \kappa}, \quad \phi = 1 \quad \text{at } z = 0 \quad \text{and} \quad \text{at } z = 1, \quad (3.14)$$

4 The steady solution

In basic state, the assumption is

$$\mathbf{u}_b = 0, \text{ whereas } p_b, \phi_b, T_b, \mathbf{H}_b, \mathbf{M}_b \text{ are functions of } z \text{ only.} \quad (4.1)$$

The equations (3.9)–(3.13), under the assumption (4.1), using bc_s (3.14), and following [25], give the solution of basic state as follows:

$$\begin{aligned} \mathbf{u}_b = 0, \quad p = p_b(z), \quad T_b = Ra(z - z^2) + \frac{\rho_f g \alpha d^3 T_0}{\mu \kappa}, \quad \phi_b = s^* Ra(z - z^2) + 1, \\ H_b = \left(\frac{M_1}{M_3} - \frac{M'_1}{M'_3} s^* \right) Ra(z - z^2) + 1, \quad M_b = -\frac{1}{\chi_2} \left(\frac{M_1}{M_3} - \frac{M'_1}{M'_3} s^* \right) Ra(z - z^2) + 1, \end{aligned} \quad (4.2)$$

$$\text{where } s^* = \left(-Na + \frac{M_1}{M_3} Na' \right) / \left(1 + \frac{M'_1}{M'_3} Na' \right).$$

5 Analysis of linear stability mechanisms

Considering the disturbances with an amplitude τ ($\tau \rightarrow 0$) to (4.1) we have:

$$\begin{aligned} \mathbf{u} = \mathbf{u}_b + \tau \mathbf{u}, \quad p = p_b + \tau p, \quad T = T_b + \tau \theta, \quad \phi = \phi_b + \tau \phi, \\ \mathbf{M} = \mathbf{M}_b + \tau \mathbf{M}, \quad \mathbf{H} = \mathbf{H}_b + \tau \mathbf{H}. \end{aligned} \quad (5.1)$$

On setting (5.1) in equations [(3.8)–(3.13)], linearizing them about basic state solution, we get

$$\begin{aligned} \frac{1}{Pr} \frac{\partial \nabla^2 w}{\partial t} = \nabla^4 w + \{ (M_3 - Ra_s M'_3 s^*) Ra(1 - 2z) \} \frac{\partial \nabla_1^2 \psi}{\partial z} + \left\{ Ra_N - \left(M_1 Ra - Ra \frac{M_3 M'_1}{M'_3} s^* \right) \right. \\ \left. \times (1 - 2z) - (Ra_N N_\phi s^* Ra(z - z^2)) s(z) \right\} \nabla_1^2 \theta + \left\{ \left(Ra \frac{M_3 M'_1}{M'_3} - Ra_s M'_1 Ra s^* \right) \right. \\ \left. \times (1 - 2z) - (Rn + Ra_N N_\phi Ra(z - z^2)) s(z) \right\} \nabla_1^2 \phi - Ta^{1/2} \frac{\partial \xi}{\partial z}, \end{aligned} \quad (5.2)$$

$$\frac{1}{Pr} \frac{\partial \xi}{\partial t} = \nabla^2 \xi + Ta^{1/2} \frac{\partial w}{\partial z}, \quad (5.3)$$

$$\frac{\partial \phi}{\partial t} = -s^* Ra(1 - 2z)w + \frac{1}{Le} \nabla^2 \phi + \frac{Na}{Le} \nabla^2 \theta - \frac{Na'}{Le} \frac{\partial}{\partial z} \nabla^2 \psi, \quad (5.4)$$

$$\begin{aligned} \frac{\partial \theta}{\partial t} = -Ra(1 - 2z)w + \nabla^2 \theta + \left\{ \frac{Nb}{Le} s^* + \frac{2NaNb}{Le} - \frac{NbNa' M_1}{Le M_3} + \frac{NbNa' M'_1}{Le M'_3} s^* \right\} \\ \times Ra(1 - 2z) \frac{\partial \theta}{\partial z} + \frac{Nb}{Le} Ra(1 - 2z) \frac{\partial \phi}{\partial z} - \frac{NbNa'}{Le} Ra(1 - 2z) \frac{\partial^2 \psi}{\partial z^2}, \end{aligned} \quad (5.5)$$

$$\frac{\partial^2 \psi}{\partial z^2} = \frac{M_1}{M_3} \frac{\partial \theta}{\partial z} - \frac{M'_1}{M'_3} \frac{\partial \phi}{\partial z} - \frac{(1 + \chi_2)}{(1 + \chi)} \nabla_1^2 \psi. \quad (5.6)$$

In order to perform the normal mode analysis, following [25], all the perturbation quantities w, θ, ϕ, ψ are assumed in the form

$$\{w, \xi, \theta, \phi, \psi\} = \{w(z), \xi(z), \theta(z), \phi(z), \psi(z)\} \exp\{\sigma t + i(k_x x + k_y y)\}, \quad (5.7)$$

On substituting (5.7) into the set of Equations (5.2)–(5.6) gives

$$\begin{aligned} \frac{\sigma}{Pr} (4D^2 - k^2)w(z) = (4D^2 - k^2)^2 w(z) - \left\{ Ra_N + \left(M_1 Ra - Ra \frac{M_3 M'_1}{M'_3} s^* \right) z \right. \\ \left. - (Ra_N N_\phi Ra s^* \frac{(1 - z^2)}{4} s \left(\frac{1 + z}{2} \right)) \right\} k^2 \theta(z) + \left\{ \left(Ra \frac{M_3 M'_1}{M'_3} - Ra_s M'_1 Ra s^* \right) z + Rn \right. \\ \left. + Ra_N N_\phi Ra \frac{(1 - z^2)}{4} s \left(\frac{1 + z}{2} \right) \right\} k^2 \phi(z) + \{ (M_3 - Ra_s M'_3 s^*) Ra \} 2k^2 z D\psi(z) - 2Ta^{1/2} D\xi, \end{aligned} \quad (5.8)$$

$$\frac{\sigma}{Pr} \xi = (4D^2 - k^2)\xi + 2Ta^{1/2} Dw, \quad (5.9)$$

$$\begin{aligned} \sigma\phi(z) = & s^* Razw(z) + \frac{1}{Le}(4D^2 - k^2)\phi(z) + \frac{Na}{Le}(4D^2 - k^2)\theta(z) \\ & - \frac{2Na'}{Le}(4D^2 - k^2)D\psi(z), \end{aligned} \quad (5.10)$$

$$\begin{aligned} \sigma\theta(z) = & Razw(z) + (4D^2 - k^2)\theta(z) - \left\{ \frac{Nb}{Le}s^* + \frac{2NaNb}{Le} - \frac{NbNa'M_1}{LeM_3} + \frac{NbNa'M'_1}{LeM'_3}s^* \right\} \\ & \times 2RaD\theta(z) - 2\frac{Nb}{Le}RazD\phi(z) + 4\frac{NbNa'}{Le}RazD^2\psi(z), \end{aligned} \quad (5.11)$$

$$\left\{ 4D^2 - \frac{k^2(1 + \chi_2)}{(1 + \chi)} \right\} \psi(z) - \frac{2M_1}{M_3}D\theta(z) + \frac{2M'_1}{M'_3}D\phi(z) = 0, \quad (5.12)$$

The considered bc_s for rigid-free (\mathcal{RF}) boundaries are as follows:

$$\left. \begin{aligned} w = Dw = \xi = \theta = D\phi = 2(1 + \chi)D\psi - k\psi = 0 & \quad \text{at } z = -1, \\ w = D^2w = D\xi = \theta = D\phi = 2(1 + \chi)D\psi + k\psi = 0 & \quad \text{at } z = +1. \end{aligned} \right\} \quad (5.13)$$

6 Method of solution

To solve the system of equations (5.8)–(5.12) under the bc_s (5.13), we use a numerical method inspired by [29]. The system is transformed into an eigenvalue problem, and MATLAB's EIG function, in conjunction with the QZ algorithm which is employed to identify the dominant eigenvalue, $\sigma = \sigma_r + i\sigma_i$, where σ_r represents the real part. The dominant eigenvalue with the largest real part, σ_r , is crucial in determining system stability.

We then apply the secant method to iteratively adjust parameters until σ_r approaches zero, which corresponds to a point on the \mathcal{N}_s Curve. This procedure is repeated for a range of wave numbers, k , to create a complete stability curve, following the methodology of [28]. This combined approach of eigenvalue analysis and iterative techniques effectively maps out the system's stability boundary.

7 Results and discussion

We present numerical profiles for $\mathcal{W}\text{-}\mathcal{MG}_{fluid}$ and $\mathcal{E}\text{-}\mathcal{MG}_{fluid}$ flows through \mathcal{RF} bc_s . The physical parameter values used in this analysis are drawn from the studies by [29] and [30]. In our approach, we examine the behavior of the system by investigating these configurations, $\mathcal{W}\text{-}\mathcal{MG}_{fluid}$ and $\mathcal{E}\text{-}\mathcal{MG}_{fluid}$, in which different magneto-fluidic parameters play a critical role. These numerical results help us understand the stability characteristics and convection patterns specific to each configuration. By implementing these parameter values from well-established sources, we ensure that our results align closely with prior theoretical and experimental findings. This analysis offers insights into how the \mathcal{RF} bc_s influence the system dynamics, shedding light on the role of each physical parameter in controlling stability and flow structure in magneto-fluid systems.

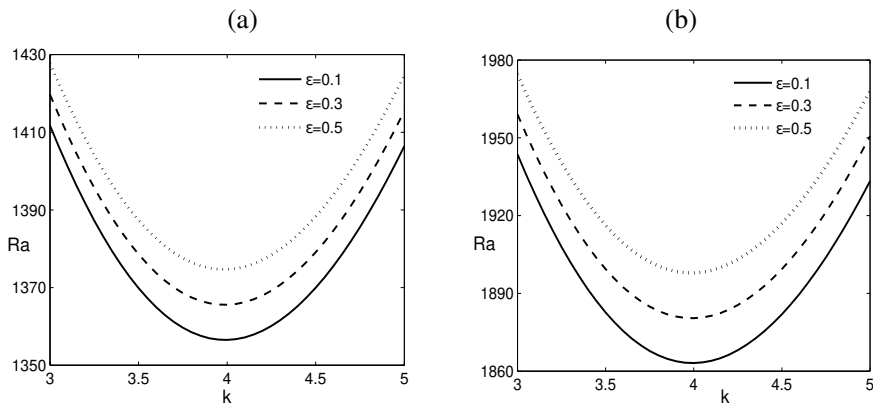


Figure 2. \mathcal{N}_s Curves for different values of variable gravity parameter ϵ for (a) $\mathcal{W}\text{-}\mathcal{MG}_{fluid}$ & (b) $\mathcal{E}\text{-}\mathcal{MG}_{fluid}$.

Figure 2 demonstrates the stabilizing influence of the variable gravity parameter, ϵ , on the system. As the value of ϵ increases, the \mathcal{N}_s Curves shifts upward, indicating a higher critical Rayleigh number, Ra_c . This increase in Ra_c reflects enhanced system stability under variable gravity conditions. The stabilizing effect arises because variable gravity induces variations in buoyancy forces, which counteract convective disturbances. Consequently, a larger ϵ makes it more difficult for instability to develop, thus requiring a higher threshold for convection to occur.

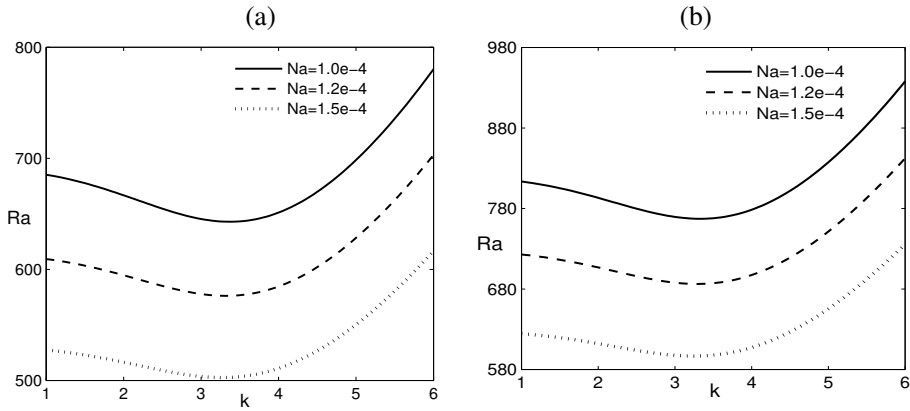


Figure 3. $\mathcal{N}_s \mathcal{C}_{curves}$ for different values of modified diffusivity ratio Na for (a) $\mathcal{W}\text{-}\mathcal{M}\mathcal{G}_{fluid}$ & (b) $\mathcal{E}\text{-}\mathcal{M}\mathcal{G}_{fluid}$.

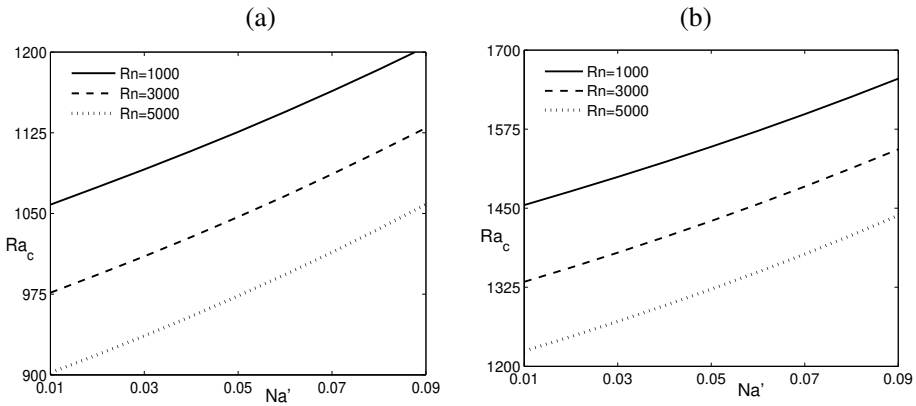


Figure 4. $\mathcal{C}_s \mathcal{C}_{curves}$ representing variation of Ra_c as a function Na' for different values Rn for (a) $\mathcal{W}\text{-}\mathcal{M}\mathcal{G}_{fluid}$ & (b) $\mathcal{E}\text{-}\mathcal{M}\mathcal{G}_{fluid}$.

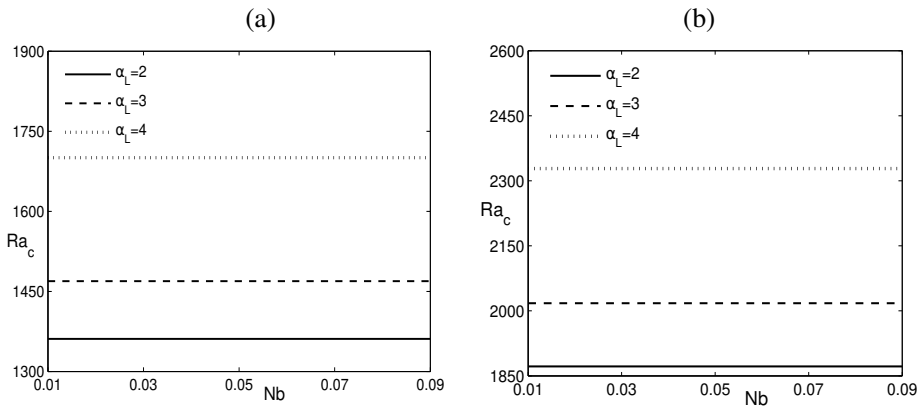


Figure 5. $\mathcal{C}_s \mathcal{C}_{curves}$ representing variation of Ra_c as a function Nb for different values α_L for (a) $\mathcal{W}\text{-}\mathcal{M}\mathcal{G}_{fluid}$ & (b) $\mathcal{E}\text{-}\mathcal{M}\mathcal{G}_{fluid}$.

Figure 3 shows that $\mathcal{N}_s \mathcal{C}_{curves}$ shifts downward with the increase of Na showing the destabilizing effect on the system of the parameter Na . This relationship arises because higher values of Na amplify thermophoretic diffusion, which subsequently drives the movement of magnetic nanoparticles. The increase in thermophoretic diffusivity generates disturbances within the $\mathcal{M}\mathcal{G}_{fluid}$, leading to a lower value of Ra_c .

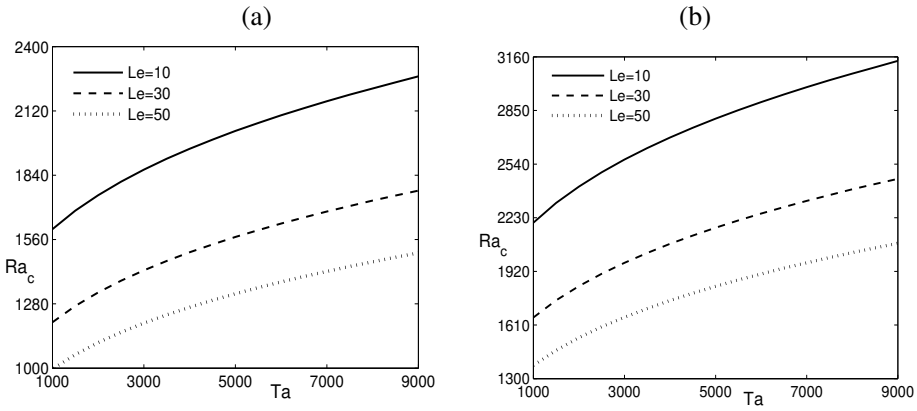


Figure 6. C_s Curves representing variation of Ra_c as a function Ta for different values Le for (a) $W-MG_{fluid}$ & (b) $E-MG_{fluid}$.

Figure 4 highlight the stabilizing effect of Na' and destabilizing impact of the parameter Rn on the system's stability. As shown in the figure, increasing Rn leads to a decrease in the critical Rayleigh number, Ra_c , which marks the onset of convection. This reduction in Ra_c occurs because higher Rn values intensify the Brownian motion of nanoparticles, enhancing particle diffusion within the fluid. The increased nanoparticle activity due to Brownian motion triggers disturbances, which promote convective instability and thus lower the stability threshold of the system. Consequently, a higher Rn results in a lower Ra_c , revealing that Rn acts as a destabilizing factor.

Figure 5 illustrates the relationship between the critical Rayleigh number, Ra_c , and the parameter Nb for three different values of the Langvein parameter, α_L . The plot shows that Ra_c remains almost unchanged as Nb increases, suggesting that Nb has a minimal impact on the onset of thermal convection. In contrast, the influence of α_L on Ra_c is much more significant. This is due to the fact that the internal heat source forces become more dominant than the magnetic forces, which reduces disturbances in the MG_{fluid} as the magnetic field strengthens. Consequently, Ra_c increases, which delays the onset of convection. In conclusion, while the parameter Nb has little effect on the critical Rayleigh number, the Langvein parameter, α_L , plays a crucial role in delaying convection by raising the critical threshold for instability in the system.

Figure 6 presents the relationship between Ra_c and the Taylor number, Ta , for three distinct values of the Lewis number, Le . The plot demonstrates the destabilizing effect of Le and the stabilizing effect of Ta . The destabilizing influence of Le arises because a higher Lewis number increases the thermal diffusivity relative to mass diffusivity, enhancing temperature gradients and promoting more intense convective motion. On the other hand, in a Newtonian fluid, rotation generates vorticity, which results in higher horizontal velocities between the plates. This increased horizontal motion reduces the vertical fluid movement, thereby delaying the onset of convection, which accounts for the stabilizing effect of the Taylor number [31].

Table 1. Values of Ra_c & k_c for $\mathcal{W}\text{-}\mathcal{M}\mathcal{G}_{fluid}$ & $\mathcal{E}\text{-}\mathcal{M}\mathcal{G}_{fluid}$.

		$\mathcal{R}\mathcal{R}\text{-boundaries}$			
		$\mathcal{W}\text{-}\mathcal{M}\mathcal{G}_{fluid}$		$\mathcal{E}\text{-}\mathcal{M}\mathcal{G}_{fluid}$	
$h(z_1)$	Ta	k_c	Ra_c	k_c	Ra_c
z_1	1000	4.4	1940	4.4	2665
	2000	4.8	2014	4.8	2767
	3000	5.0	2074	5.0	2851
	4000	5.3	2125	5.3	2923
	5000	5.5	2169	5.4	2985
	6000	5.6	2207	5.6	3041
	7000	5.7	2242	5.7	3091
	8000	5.9	2273	5.8	3137
	9000	6.0	2302	5.9	3179
	10000	6.0	2328	6.0	3218
$-z_1$	1000	4.3	1959	4.4	2705
	2000	4.7	2034	4.8	2807
	3000	5.0	2095	5.0	2892
	4000	5.3	2146	5.3	2963
	5000	5.5	2189	5.5	3025
	6000	5.6	2227	5.6	3080
	7000	5.8	2260	5.7	3129
	8000	5.9	2291	5.8	3174
	9000	6.0	2319	5.9	3215
	10000	6.1	2345	6.0	3253
$-z_1^2$	1000	4.3	1957	4.4	2699
	2000	4.7	2031	4.8	2802
	3000	5.0	2092	5.0	2886
	4000	5.3	2143	5.3	2958
	5000	5.5	2186	5.4	3020
	6000	5.6	2224	5.6	3075
	7000	5.8	2258	5.7	3124
	8000	5.9	2289	5.8	3169
	9000	6.0	2317	5.9	3210
	10000	6.1	2343	6.0	3249

Tables (1-3) present the values of k_c and Ra_c as a function of the Taylor number, Ta , under different gravity variations, namely z_1 , $-z_1$, and $-z_1^2$. These values are calculated for $\mathcal{W}\text{-}\mathcal{M}\mathcal{G}_{fluid}$ and $\mathcal{E}\text{-}\mathcal{M}\mathcal{G}_{fluid}$, across three distinct boundary conditions: Rigid–Rigid ($\mathcal{R}\mathcal{R}$), Rigid–Free ($\mathcal{R}\mathcal{F}$), and Free–Free ($\mathcal{F}\mathcal{F}$). The tables reveal that Ra_c is highest when both boundaries are rigid and lowest when both boundaries are free, indicating that the system is most stable with rigid boundaries and least stable with free boundaries. Furthermore, the data show a consistent trend where both k_c and Ra_c increase as the Taylor number, Ta , rises, regardless of the boundary conditions. This suggests that as Ta increases, the system’s stability is enhanced, delaying the onset of penetrative convection. Additionally, the increase in Ta results in a reduction in the cell size, further affecting the convection dynamics. Thus, Ta plays a significant role in modulating the onset of convection and the size of the convective cells.

Table 2. Values of Ra_c & k_c for $\mathcal{W}\text{-}\mathcal{MG}_{fluid}$ & $\mathcal{E}\text{-}\mathcal{MG}_{fluid}$.

		$\mathcal{RF} - boundaries$			
		$\mathcal{W}\text{-}\mathcal{MG}_{fluid}$		$\mathcal{E}\text{-}\mathcal{MG}_{fluid}$	
$h(z_1)$	Ta	k_c	Ra_c	k_c	Ra_c
z_1	1000	4.0	1343	4.0	1838
	2000	4.5	1482	4.5	2032
	3000	4.9	1585	4.9	2177
	4000	5.2	1670	5.2	2295
	5000	5.5	1741	5.5	2396
	6000	5.7	1804	5.7	2484
	7000	5.9	1861	5.9	2563
	8000	6.0	1912	6.0	2635
	9000	6.2	1960	6.2	2702
	10000	6.3	2003	6.3	2763
$-z_1$	1000	4.0	1361	4.0	1872
	2000	4.5	1500	4.5	2066
	3000	4.9	1603	4.9	2211
	4000	5.2	1687	5.2	2329
	5000	5.5	1759	5.5	2429
	6000	5.7	1822	5.7	2518
	7000	5.9	1879	5.9	2597
	8000	6.0	1930	6.0	2669
	9000	6.2	1977	6.2	2735
	10000	6.3	2020	6.3	2796
$-z_1^2$	1000	4.0	1359	4.0	1867
	2000	4.5	1498	4.5	2062
	3000	4.9	1601	4.9	2207
	4000	5.2	1685	5.2	2325
	5000	5.5	1757	5.5	2425
	6000	5.7	1820	5.7	2514
	7000	5.9	1876	5.9	2593
	8000	6.0	1928	6.0	2665
	9000	6.2	1975	6.2	2731
	10000	6.3	2018	6.3	2792

Table 3. Values of Ra_c & k_c for $\mathcal{W}\text{-}\mathcal{MG}_{fluid}$ & $\mathcal{E}\text{-}\mathcal{MG}_{fluid}$.

		<i>FF-boundaries</i>			
		$\mathcal{W}\text{-}\mathcal{MG}_{fluid}$		$\mathcal{E}\text{-}\mathcal{MG}_{fluid}$	
$h(z_1)$	Ta	k_c	Ra_c	k_c	Ra_c
z_1	1000	4.0	1346	4.0	1847
	2000	4.1	1482	4.4	2040
	3000	4.7	1590	4.9	2186
	4000	5.2	1676	5.2	2305
	5000	5.5	1748	5.5	2406
	6000	5.8	1811	5.7	2494
	7000	6.0	1866	5.9	2572
	8000	6.1	1916	6.1	2642
	9000	6.3	1961	6.3	2707
	10000	6.4	2003	6.4	2766
$-z_1$	1000	4.0	1361	4.0	1877
	2000	4.0	1493	4.2	2069
	3000	4.5	1604	4.8	2218
	4000	5.1	1693	5.2	2338
	5000	5.5	1766	5.5	2439
	6000	5.8	1828	5.8	2527
	7000	6.0	1883	6.0	2605
	8000	6.2	1932	6.1	2675
	9000	6.3	1977	6.3	2738
	10000	6.4	2019	6.4	2798
$-z_1^2$	1000	4.0	1359	4.0	1873
	2000	4.0	1492	4.3	2066
	3000	4.6	1602	4.8	2214
	4000	5.1	1691	5.2	2334
	5000	5.5	1764	5.5	2435
	6000	5.8	1826	5.7	2523
	7000	6.0	1881	6.0	2601
	8000	6.2	1930	6.1	2671
	9000	6.3	1975	6.3	2735
	10000	6.4	2017	6.4	2794

8 Conclusions

In this study, we explored how variable gravity influences the initiation of penetrative convection driven by internal heating within a rotating thin layer of \mathcal{MG}_{fluid} under the effect of an external magnetic field. The main findings are as follows. The parameters, namely, ϵ , α_L , Na , and Ta were found to delay the onset of convection, thereby enhancing the system's stability. Conversely, parameters Na , Le , and Rn promote convection, whereas Nb has a minimal impact. As Ta increases, the size of convection cells decreases. This relationship suggests that smaller cell sizes contribute to a more stable system. The system achieves maximum stability under \mathcal{RR}_{bc_s} and minimum stability under \mathcal{FF}_{bc_s} boundary conditions. Furthermore, the \mathcal{E} - \mathcal{MG}_{fluid} configuration demonstrates slightly higher stability than the \mathcal{W} - \mathcal{MG}_{fluid} configuration. These insights advance our understanding of how variable gravity, boundary conditions, and other parameters affect the onset of penetrative convection in a rotating \mathcal{MG}_{fluid} , offering valuable perspectives for enhancing stability in such fluid systems.

References

- [1] W. Yu and H. Xie, *A review on nanofluids: preparation, stability mechanisms, and applications*, Journal of Nanomaterials, **2012**, 1–17, (2012).
- [2] R. Sekar and G. Vaidyanathan, *Convective instability of a magnetized ferrofluid in a rotating porous medium*, International journal of engineering science, **31(8)**, 1139–1150, (1993).
- [3] Sunil and A. Mahajan, *A nonlinear stability analysis for rotating magnetized ferrofluid heated from below saturating a porous medium*, Zeitschrift für angewandte Mathematik und Physik, **60(2)**, 344–362, (2009).
- [4] J. Buongiorno, *Convective transport in nanofluids*, Journal of Heat Transfer, **128**, 240–250, (2006).
- [5] D.A. Nield and A.V. Kuznetsov, *Thermal instability in a porous medium layer saturated by a nanofluid*, International Journal of Heat and Mass Transfer, **52(25)**, 5796–5801, (2009).
- [6] D. A. Nield, and A. V. Kuznetsov, *Thermal instability in a porous medium layer saturated by a nanofluid: a revised model*, International Journal of Heat and Mass Transfer, **68**, 211–214, (2014).
- [7] B.S. Bhadauria and S. Agarwal, *Natural convection in a nanofluid saturated rotating porous layer: a nonlinear study*, Transport in Porous Media, **87(2)**, 585–602, (2011).
- [8] S. Agarwal and B.S. Bhadauria, *Natural convection in a nanofluid saturated rotating porous layer with thermal non-equilibrium model*, Transport in porous media, **90(2)**, 627–654, (2011).
- [9] S. Agarwal, B.S. Bhadauria and P.G. Siddheshwar, *Thermal instability of a nanofluid saturating a rotating anisotropic porous medium*, Special Topics and Reviews in Porous Media: An International Journal, **2(1)**, 53–64, (2011).
- [10] R. Chand and G.C. Rana, *On the onset of thermal convection in rotating nanofluid layer saturating a Darcy–Brinkman porous medium*, International Journal of Heat and Mass Transfer, **55(21)**, 5417–5424, (2012).
- [11] R. D. Gasser and M. S. Kazimi, *Onset of convection in a porous medium with internal heat generation*, ASME J. Heat Transfer, **98**, 49–54, (1976).
- [12] K. A. Ames and Shannon S. Cobb, *Penetrative convection in a porous medium with internal heat sources*, International journal of engineering science, **32**, 95–105, (1994).
- [13] K. A. Ames and B. Straughan, *Penetrative convection in fluid layers with internal heat sources*, Acta mechanica, **85(3–4)**, 137–148, (1990).
- [14] S. Rionero and B. Straughan, *Convection in a porous medium with internal heat source and variable gravity effects*, International Journal of Engineering Science, **28(6)**, 497–503, (1990).
- [15] M. Carr, *Penetrative convection in a superposed porous-medium-fluid layer via internal heating*, Journal of Fluid Mechanics, **509**, 305–329, (2004).
- [16] B. Straughan, *The energy method, stability and nonlinear convection*, Springer–Verlag New York, (2004).
- [17] F. Capone, M. Gentile and A. A. Hill, *Penetrative convection via internal heating in anisotropic porous media*, Mechanics Research Communications, **37(5)**, 441–444, (2010).
- [18] D. Yadav, J. Lee and H. H. Cho, *Brinkman convection induced by purely internal heating in a rotating porous medium layer saturated by a nanofluid*, Powder Technology, **286**, 592–601, (2015).
- [19] C. E. Nanjundappa, M. Ravisha, J. Lee and I. S. Shivakumara, *Penetrative ferroconvection in a porous layer*, Acta Mechanica, **216**, 243–257, (2011).
- [20] A. Harfash, *Convection in a porous medium with variable gravity field and magnetic field effects*, Transport in porous media, **103(3)**, 361–379, (2014).
- [21] S. M. Alex and P. R. Patil, *Effect of variable gravity field on solet driven thermosolutal convection in a porous medium*, International communications in heat and mass transfer, **28(4)**, 509–518, (2001).
- [22] P. Kaloni and Z. Qiao, *Non-linear convection in a porous medium with inclined temperature gradient and variable gravity effects*, International journal of heat and mass transfer, **44(8)**, 1585–1591, (2001).
- [23] R. Chand, G. Rana and S. Kumar, *Variable gravity effects on thermal instability of nanofluid in anisotropic porous medium*, International Journal of Applied Mechanics and Engineering, **18(3)**, 631–642, (2013).

- [24] R. Chand, G. Rana and S. Kango, *Effect of variable gravity on thermal instability of rotating nanofluid in porous medium*, FME Transactions, **43(1)**, 62–69, (2015).
- [25] A. Mahajan and M. K. Sharma, *Penetrative convection in a rotating internally heated magnetic nanofluid layer*, Journal of Nanofluids, **8(1)**, 187-198, (2019)
- [26] A. Mahajan and M. K. Sharma, *The onset of convection in a magnetic nanofluid layer with variable gravity effects*, Applied Mathematics and Computation, **339**, 622-635, (2018).
- [27] B.A. Finlayson, *Convective instability in ferromagnetic fluids*, J Fluid Mech, **40**, 753–767, (1970).
- [28] A. Mahajan and M. K. Sharma, *Penetrative convection in magnetic nanofluids via internal heating*, The Physics of fluids, **29**, 034101, (2017).
- [29] P. N. Kaloni and J. X. Lou, *Convective instability of magnetic fluids*, Physical Review E, **70**, 026313, (2004).
- [30] R. E. Rosensweig, *Ferrohydrodynamics*, Courier Dover Corporation, (1972).
- [31] S. Chandrasekhar, *Hydrodynamic and hydromagnetic stability*, Courier Corporation, (2013).

Author information

M. Arora, Department of Mathematics, Lovely Professional University, Phagwara, Punjab, India.

E-mail: monikaarora1879@gmail.com

M.K. Sharma, Department of Mathematics, Maharaja Agrasen University, Baddi, Himachal Pradesh, India.

E-mail: mksharma.maths@gmail.com